Modulation of Connectivity in Visual Pathways by Attention: Cortical Interactions Evaluated with Structural Equation Modelling and fMRI

Christian Büchel and Karl J. Friston

The Wellcome Department of Cognitive Neurology, Institute of Neurology, Queen Square, London WC1N 3BG, UK

Electrophysiological and neuroimaging studies have shown that attention to visual motion can increase the responsiveness of the motion-selective cortical area V5 and the posterior parietal cortex (PP). Increased or decreased activation in a cortical area is often attributed to attentional modulation of the cortical projections to that area. This leads to the notion that attention is associated with changes in connectivity. We have addressed attentional modulation of effective connectivity using functional magnetic resonance imaging (fMRI). Three subjects were scanned under identical stimulus conditions (visual motion) while varying only the attentional component of the task. Haemodynamic responses defined an occipito-parieto-frontal network, including the, primary visual cortex (V1), V5 and PP. A structural equation model of the interactions among these dorsal visual pathway areas revealed increased connectivity between V5 and PP related to attention. On the basis of our analysis and the neuroanatomical pattern of projections from the prefrontal cortex to PP, we attributed the source of modulatory influences, on the posterior visual pathway, to the prefrontal cortex (PFC). To test this hypothesis we included the PFC in our model as a 'modulator' of the pathway between V5 and PP, using interaction terms in the structural equation model. This analysis revealed a significant modulatory effect of prefrontal regions on V5 afferents to posterior parietal cortex.

Introduction

Functional neuroimaging has been extremely successful in establishing functional segregation as a principle of organization in the human brain. More recent approaches to understanding the data have focused on the integration of functionally segregated areas through characterizing neurophysiological activations in terms of distributed changes. These approaches have introduced a number of concepts (e.g. functional and effective connectivity) and their application to issues in imaging neuroscience (e.g. functional integration and non-linear cortical interactions) (Horwitz *et al.*, 1991; McIntosh and Gonzalez-Lima, 1991; Friston *et al.*, 1993a,b; Lagreze *et al.*, 1993; McIntosh *et al.*, 1996a). The present work represents a further step in using neuroimaging to characterize functional integration in the brain.

The hypothesis that attention can be expressed as a modulation or change in effective connectivity is captured in a quotation by LaBerge (1995): 'The expression of attention in a brain area appears to be described effectively as an enhancement of activity in the attended set of pathways relative to the unattended set of pathways.' Functional neuroimaging has been used to infer modulation of extrastriate cortical areas by attentional processes (Corbetta *et al.*, 1991; O'Craven and Savoy, 1997). Electrophysiological and functional magnetic resonance imaging (fMRI) studies have identified neuronal responses attributable to attentional processing at the level of the posterior parietal cortex (Bushnell *et al.*, 1981; Mesulam, 1981; Mountcastle *et al.*, 1981; Assad and Maunsell, 1995). Recent

results (Treue and Maunsell, 1996) demonstrate attentional modulation at the level of V5 in primates. Inferences about modulation in these studies were based on regionally specific changes in activity (i.e. BOLD contrast in fMRI or neuronal activity in single-cell electrophysiology). However, the modulation of pathways can be characterized explicitly in terms of changes in effective connectivity among cortical areas.

In neuroimaging functional connectivity is defined as the temporal correlation between remote neurophysiological events, whereas effective connectivity is defined as the influence one neural system exerts over another (Friston *et al.*, 1993b, 1995e). Functional connectivity is simply a statement about the observed correlations; it does not provide any direct insight into how these correlations are mediated. To clarify the distinction between functional and effective connectivity let us consider a simple example. The mediodorsal nucleus of the thalamus is interconnected with different cortical areas. Increased activity in this structure will therefore lead to highly correlated brain activity in the cortical terminal fields of its projections, despite the fact that the cortical areas may not be directly connected. Eigenimage analysis (i.e. an analysis based on functional connectivity) of the cortical data, without the thalamus, would reveal a functional network of cortical areas. This example highlights the teleological weakness of functional connectivity and speaks of the importance of modelling interactions using effective connectivity.

The concept of effective connectivity was originated in the analysis of separable spike trains obtained from multi-unit electrode recordings (Gerstein and Perkel, 1969; Gerstein *et al.*, 1989; Aertsen and Preissl, 1991; Gochin *et al.*, 1991). Effective connectivity is closer to the intuitive notion of a connection than functional connectivity and can be defined as the influence one neural system exerts over another (Friston *et al.*, 1995e), either at a synaptic (cf. synaptic efficacy) or cortical level. In electrophysiology there is a close relationship between effective connectivity and synaptic efficacy.

Although functional and effective connectivity can be invoked at a conceptual level in both neuroimaging and electrophysiology, they differ fundamentally at a practical level. This is because the timescales and nature of the neurophysiological measurements are very different (seconds versus milliseconds and haemodynamic versus spike trains). In electrophysiology it is often necessary to remove the confounding effects of stimulus-locked transients (which introduce correlations not causally mediated by direct neural interactions) in order to reveal the underlying connectivity. The confounding effect of stimulus-evoked transients is less problematic in neuroimaging because the promulgation of dynamics from primary sensory areas onwards is mediated by neuronal connections (usually reciprocal and interconnecting). In other words in functional

imaging, stimulus-related transients in higher areas *must* be mediated by connectivity from lower areas.

One method used to estimate effective connectivity is structural equation modelling. This technique combines an anatomical (constraining) model and the inter-regional covariances of activity. The ensuing functional model represents the influence of regions on each other through the putative anatomical connections.

Structural equation modelling is a linear technique and therefore cannot model non-linear context or activity-dependent changes in connection strength (i.e. modulation). However, this problem can be circumnavigated, by comparing two models, one where the modulatory influence is present and one where it is absent. The more compelling alternative is to specify a new variable within the model, comprising a (second-order) term that models the interaction between an input to a region and modulatory afferents. This can be compared with modulation at a synaptic level, where a neuronal afferent can modulate the 'gain' of a synaptic connection.

In this paper we present fMRI data from three individual subjects, scanned under identical stimulus conditions, and changing only the attentional component of the tasks employed. In the first stage we identified regions that showed differential activations in relation to attentional set. In the second stage changes in effective connectivity between these areas were assessed using structural equation modelling (McIntosh *et al.*, 1994). In the final stage we show how these attention-dependent changes in effective connectivity can be explained by modulation, of the dorsal visual pathway, by frontal cortical areas. These effects are characterized by extending standard structural equation modelling to include non-linear interaction terms or moderators (Kenny and Judd, 1984). We also demonstrate the regional specificity of the interaction (i.e. modulation) and give an intuitive illustration of modulation using a simple regression analysis. The methods section of the paper is divided into three sections. Firstly we introduce structural equation modelling. We then describe how we identified those regions involved in attentional processing and finally introduce the neuroanatomical model used in the analysis.

Materials and Methods

Structural Equation Modelling
Structural equation modelling or path analysis is a technique developed in economics, psychology and the social sciences. The basic idea differs from the usual statistical approach of modelling individual observations. In multiple regression or ANOVA the regression coefficients or parameters of the model are based on the minimization of the sum of squared differences between the predicted and observed dependent variables. Structural equation modelling approaches the data from a different perspective. Instead of considering variables individually, the emphasis is on the covariance structure. Parameters are estimated in structural equation modelling by minimizing the difference between the observed covariances and these implied by a structural or path model (see Appendix for operational equations). The parameters of the model are connection strength or path coefficients and correspond to an estimate of effective connectivity. McIntosh and Gonzales-Lima (1994) used structural equation modelling to demonstrate the dissociation between ventral and dorsal visual pathways for object and spatial vision with positron emission tomography (PET) data in the human. Grafton and colleagues used structural equation modelling to assess the effect of pallidotomy on effective connectivity in the motor system of Parkinson patients (Grafton *et al.*, 1994). Recently structural equation modelling was used to characterize changes in effective connectivity during memory tasks (McIntosh *et al.*, 1996b; Nyberg *et al.*, 1996)

In terms of neural systems a measure of covariance represents the

degree to which the activities of two or more regions are related. The study of covariance structures in neuroimaging has a unique advantage compared to applications in other fields: the interconnections among the dependent variables (regional activity of brain areas) are anatomically determined and the activation of each region can be measured directly. This is in contrast to 'classical' structural equation modelling in the behavioural sciences, where, sometimes, the models are hypothetical or 'latent' and cannot be assessed directly.

Anatomical Model
An important issue in structural equation modelling is the determination of the underlying anatomical model. This model comprises regions and connections between those regions. Different methods can be combined to identify important regions: categorical comparisons between different conditions and eigenimages highlighting structures of functional connectivity, in conjunction with results from primate electrophysiology have been used (McIntosh and Gonzalez-Lima, 1991; Grafton *et al.*, 1994). The connectivity between the identified regions is mostly based on neuroanatomical tracer studies in primates. A model is always a simplification of reality. In the context of effective connectivity one has to find a compromise between complexity, anatomical accuracy and interpretability. There are also mathematical constraints on the model. If the number of free parameters (unknowns) exceeds the number of observed covariances, the system is underdetermined and no single solution exists.

Statistical Inference
Statistical inference in structural equation modelling can address two points. The goodness of the overall fit of the model, i.e. how significantly different are the implied and observed covariance structures, and the difference between alternative models (nested or stacked model approach). In the context of multivariate, normally distributed variables the minimum of the maximum likelihood function (used to estimate the free parameters) times the number of observations minus one, follows a χ^2 distribution with $(q/2)(q + 1) - p$ degrees of freedom (Bollen, 1989). p is the number of free parameters and q is the number of observed variables. In the context of the stacked model the χ^2 statistic difference test can be used to compare two models (e.g. data from different groups or conditions) in the context of structural equation modelling (Grafton *et al.*, 1994). A so-called 'null-model' is constructed where the estimates of some parameters (i.e. path coefficients) are constrained to be zero or equal for both groups. The alternative model allows these parameters to differ between the groups. The significance of the difference between the models is expressed by the difference in the χ^2 goodness of fit indicator (χ^2 difference test or likelihood ratio test; Bollen, 1989). This χ^2 statistic has n degrees of freedom, where n is the difference in the degrees of freedom between the null-model and the one in question. For example, if the null-model constrains one parameter to be equal between groups, the resulting degree of freedom for the χ^2 statistic would be one.

Path Coefficients
How are path coefficients interpreted? The path coefficient represents the response of the dependent variable to a unit change in an explanatory variable, whilst the other variables in the model are held constant (Bollen, 1989). It is also possible to standardize path coefficients with the ratio of the standard deviations of the two connected variables (the standard deviation of the caused variable constituting the denominator). This standardized coefficient can be interpreted as the response, in units of standard deviation, of the dependent variable for a standard deviation change in the explanatory variable.

Non-linear Interaction Terms
Current applications of structural equation modelling generally use linear models. However, it is possible to incorporate additional variables containing a non-linear function [e.g. $f(x) = x^2$] of the original variables (Kenny and Judd, 1984). Interactions between variables can be incorporated in a similar fashion; wherein a new variable, containing the product of two interacting variables, is introduced as an additional influence. Although the time series are normalized, the product of two variables (say V5 and PFC) will still show some correlation with the

A
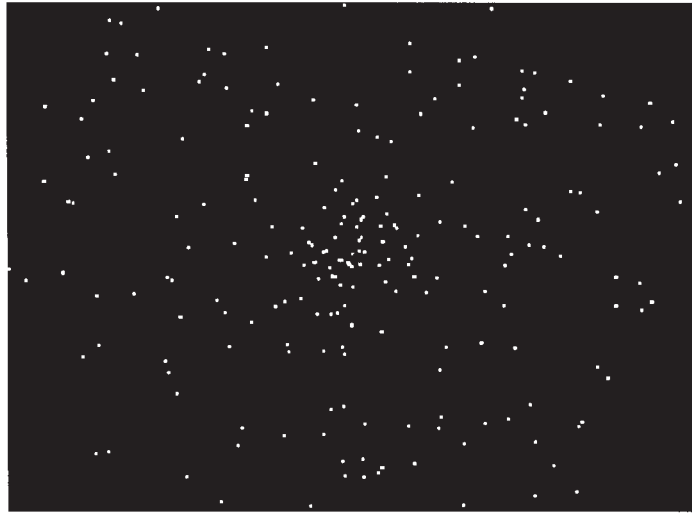
B

Run 1										Run 2								
Condition	M	F	A	F	N	F	A	F	N	S	M	F	A	F	N	F	A	F	N	S
Volumes	10	10	10	10	10	10	10	10	10	10	10	10	10	10	10	10	10	10	10
Time (s)	32	32	32	32	32	32	32	32	32	32	32	32	32	32	32	32	32	32	32

Run 3 (counterbalanced)										Run 4 (counterbalanced)								
Condition	M	F	N	F	A	F	N	F	A	S	M	F	N	F	A	F	N	F	A	S
Volumes	10	10	10	10	10	10	10	10	10	10	10	10	10	10	10	10	10	10	10
Time (s)	32	32	32	32	32	32	32	32	32	32	32	32	32	32	32	32	32	32	32

Figure 1. Stimulus as seen by the subject and experimental design. The stimulus during the 'no attention' and 'attention' conditions (*A*). Two hundred and fifty white dots (size 0.1°) were moving radially from a fixation point (size 0.3°) towards the border of the screen (17° diameter) at a constant speed of 4.7°/s. During the 'fixation' condition only the fixation mark was visible. (*B*) Experimental design. Each subject was scanned over four blocks. M denotes the first 10 discarded scans of each block with magnetic saturation effects. F, 'fixation'; A, 'attention', N, 'no attention'; S, 'stationary' condition. Each condition lasted 32 s, corresponding to 10 volume images (see Materials and Methods for a description of the conditions).

individual terms. Therefore one can residualize the product $P_{V5, PFC}$ = V5 × PFC using least squares (equation 1) to give an interaction term $I_{V5, PFC}$ that is orthogonal to V5 and PFC. This procedure can be compared to partial correlation analysis, where the effect of the established predictors is removed from a new predictor to assess the improvement in fit.

$$P_{V5, PFC} = [\mathbf{V5\ PFC}].\mathbf{b} + I_{V5, PFC}$$

i.e.

$$I_{V5, PFC} = P_{V5, PFC} - [\mathbf{V5\ PFC}]\,([\mathbf{V5\ PFC}]^T.[\mathbf{V5\ PFC}])^{-1}.[\mathbf{V5\ PFC}]^T.P_{V5, PFC} \quad (1)$$

where [**V5 PFC**] denotes a matrix containing the time-series of V5 and PFC as column vectors, and **b** is a 2 × 1 vector, containing regression coefficients. The resulting time-series of $I_{V5, PFC}$ can be seen as the residual time-series after regressing the term $P_{V5, PFC}$ on the main effects, V5 and PFC.

Even if the variables are multinormally distributed, the product of two such variables is not. Under these circumstances, maximum likelihood estimators (ML) are still consistent, but the χ^2 fit index and tests of

statistical significance may not be valid (Bollen, 1989). To overcome this problem, parameters can be estimated by weighted least squares (WLS) (Browne, 1984; Kenny and Judd, 1984) (see Appendix). As we used non-linear interaction terms in the second part of our analysis, the parameters were estimated using WLS, whereas the path coefficients in our linear models were estimated by ML.

Experimental Design and Image Acquisition

The experiment was performed on a 2 Tesla Magnetom VISION (Siemens, Erlangen) whole-body MRI system equipped with a head volume coil. Contiguous multislice $T_2{}^*$-weighted fMRI images (T_E = 40 ms; 90 ms/image; 64 × 64 pixels [19.2 × 19.2 cm]) were obtained with echo-planar imaging (EPI) using an axial slice orientation. A $T_2{}^*$-weighted sequence was chosen to enhance blood oxygenation level dependent (BOLD) contrast. The volume acquired covered the whole brain except for the lower half of the cerebellum and the most inferior part of the temporal lobes (32 slices; slice thickness 3 mm, giving 9.6 cm vertical field of view). The effective repetition time was 3.22 s.

Subjects were scanned during four runs, each lasting 5 min 22 s. One hundred image volumes were acquired in each run. Each condition lasted
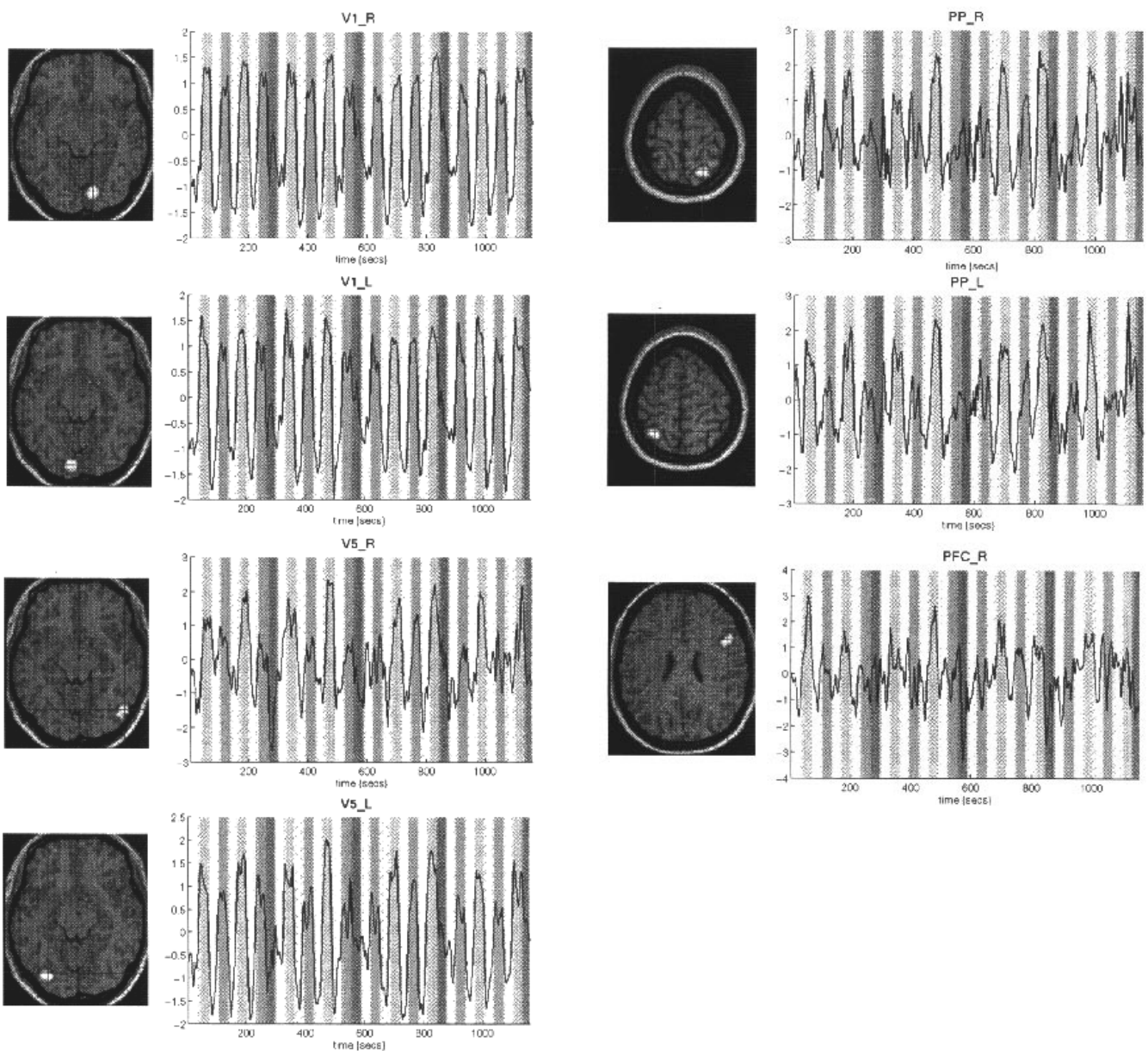
Figure 2. Spatial localization and time-course of activation for regions of interest. Regions of interest for a single subject superimposed on the T1 weighted MRI. The time course for all regions of interest is shown. The different shades of the background code different conditions (see Fig. 1*B*).

Table 1

Location of regions of interest for path analysis

Area	Subject 1		Subject 2		Subject 3	
	Location	*F* statistic	Location	*F* statistic	Location	*F* statistic
V1 R	0, −93, 0[a]	254	12, −81, −9	199	15, −96, 15	160
V1 L	0, −93, 0[a]	254	−9, −90, −12	142	−18, −93, 6	205
V5 R	42, −84, 9	77	51, −72, −12	41	45, −63, −6	55
V5 L	−36, −87, 9	111	−33, −78, −12	99	−54, −72, 3	123
PP R	21, −69, 60	43	21, −57, 66	42	24, −69, 60	52
PP L	−21, −60, 63	36	−30, −54, 60	47	−18, −69, 54	27
PFC R	57, 21, 24	21	48, 12, 24	20	51, 9, 30	14

Coordinates and the *F* statistic for each region included in the structural equation models. The maximum activation of V1 showed no lateralization in one subject, therefore the same region is used for both hemispheres. The maximum of each region was significant at $P < 0.05$ (corrected).

[a]Maximum in the midline.

32.2 s, giving 10 multislice volumes per condition. During all conditions the subjects looked at a fixation point (size 0.3°) in the middle of a transparent screen. Images were backprojected on the screen by an LCD video-projector. In conditions with visual motion 250 white dots (size 0.1°) moved radially from the fixation point in random directions towards the border of the screen, at a constant speed of 4.7°/s, where they vanished (Fig. 1A). The active screen area was circular with a diameter of 17°. The screen refresh rate was set to 67/s.

Before scanning, subjects were exposed to five 30 s trials of the stimulus. The speed of the moving dots was changed five times during each trial. Subjects were asked to indicate any change in speed. Changes in speed were gradually reduced over the trials (7, 5, 3, 2%), until a 1% change was presented on the last occasion. A 1% change in the initial speed of 4.7°/s is equivalent to a difference of 0.047°/s. We did not characterize performance in any psychophysical detail. However, during easy trials (7 and 5%) subjects performed at 100%. During the more difficult complicated trials (3, 2 and 1%) subjects continued to detect four or five changes in speed which did not coincide with the actual changes in speed. Once in the scanner, changes in speed were completely eliminated, so that identical visual stimuli were shown in all motion conditions. Four conditions – 'fixation', 'attention', 'no attention' and 'stationary' – were used (Fig. 1B). During the 'attention' and 'no attention' conditions subjects fixated centrally, while white dots emerged from the fixation point to the edge of the screen. During 'fixation' the screen was dark with only the fixation dot visible. The difference between the visual motion conditions lay in the explicit instructions given to the subjects. In the 'attention' condition the instruction was 'detect changes' and during the 'no attention' condition the subjects were instructed to 'just look'. The verbal commands were digitally recorded and played 10 s before the condition started. There were no verbal or tactile responses required.

The behavioural data were obtained by asking subjects to estimate the number of changes in speed *after* the experiment. We avoided asking subjects after each run, because of the implicit demands that would have been placed on working memory. Other ways of indicating changes on-line (e.g. button press) were dismissed because response-associated movements and their preparation would have confounded premotor (e.g. occulo-motor) responses, known to be involved in attentional processing (Rizzolatti *et al.*, 1987).

All the subjects were debriefed after the experiment and all of them told us that they detected between four and five changes in speed during the 'attention' conditions. All three subjects were rather surprised when we told them that speed changes had been eliminated.

Each run was preceded by 10 scans of a blank screen to eliminate magnetic saturation effects and then started with a 'fixation' task, followed by 'attention' , 'fixation', 'no attention' and so on. Each run of scanning ended with the fourth condition 'stationary', which consisted of the fixation point and 250 stationary dots. To avoid habituation effects the third and fourth runs were counterbalanced, starting with a 'no attention' condition instead of an 'attention' condition. There was a gap of 5 min between each run while the scanner image processor reconstructed the images.

Image Analysis and Categorical Comparisons
Image processing and statistical analysis were carried out using SPM96 (Worsley and Friston, 1995; Friston *et al.*, 1995c, 1996). All volumes were realigned to the first volume (Friston *et al.*, 1995a). A mean image was created using the realigned volumes. A structural MRI, acquired using a standard three-dimensional T_1 weighted sequence ($1 \times 1 \times 3$ mm voxel size), was co-registered to this mean (T_2^*) image. Finally all the images were spatially normalized (Friston *et al.*, 1995a) to a standard template (Talairach and Tournoux, 1988; Evans *et al.*, 1993). The data were smoothed using a 6 mm full width at half maximum isotropic Gaussian kernel. Data analysis was performed by modelling the different conditions ('attention', 'no attention', 'fixation' and 'stationary') as reference waveforms in the context of the general linear model as employed by SPM96 (Friston *et al.*, 1995b). Specific effects were tested with appropriate linear contrasts of the parameter estimates for each condition, resulting in a *t*-statistic for each and every voxel. These *t*-statistics (transformed to *Z*-statistics) constitute a statistical parametric map (SPM). These SPMs are then interpreted by referring to the probabilistic behaviour of Gaussian random fields. Data were analysed for each subject individually. The threshold adopted was $P < 0.05$ (corrected for multiple comparisons).

We used comparisons between 'attention' and 'no attention', to identify regions that showed differential responses due to attentional set. To identify regions important in early visual processing, we used the comparison between conditions involving visual motion and 'fixation'.

Identification of Regions of Interest
Regions of interest were defined by categorical comparisons using the SPM{Z} comparing 'attention' and 'no attention' and comparing 'no attention' and 'stationary'. With a stimulus consisting of radially moving dots we predicted the involvement of primary visual cortex (V1), V5, the human analogue of the middle temporal area MT of the macaque and the posterior parietal complex. The location of V1 was coincident with the calcarine fissure (Zeki *et al.*, 1991), and the location of V5 was in accord with previous functional imaging studies (Zeki *et al.*, 1991; Watson *et al.*, 1993; Tootell *et al.*, 1995). The location of the posterior parietal region was similar to that in previous PET studies of attention (Corbetta *et al.*, 1991; Coull *et al.*, 1996; Vandenberghe *et al.*, 1996). The exact coordinates and the *F*-statistic of the maximum in each region are given in Table 1. Each region was defined using a region of interest (ROI) with a diameter of 8 mm, centred around the most significant ($P < 0.05$, corrected) voxel as revealed by the categorical comparison. Figure 2 shows the location of ROIs for a single individual. A single time-series, representative of this region, was defined by the first eigenvector (identified by a singular value decomposition) of all the voxel time-series in the ROI. This denoising technique is equivalent to using the first principal component time-series of the ROI (see Sadasivan and Dutt, 1996, for a related application in EEG).

All the time-series were adjusted for confounds (e.g. global mean, low-frequency components) after applying the general linear model with condition specific predictors (Friston *et al.*, 1995d). Since our scanning protocol used sequential axial slice acquisition in descending order, signals in different slices were measured at different time points. A T_R of 3.2 s for 32 slices and a vertical field of view of 9.6 cm can therefore lead to a sampling lag of ~2 s. To correct for this, we interpolated and resampled the data. This can be seen as moving the time-series backwards or forwards in time to remove artefactual temporal differences.

Results

Changes in Effective Connectivity Related to 'Attention' Versus 'No Attention'
The dorsal visual pathway was subject to a path analysis. Our model included the primary visual cortex (V1), V5 and the posterior parietal complex (PP). Although connections between regions are generally reciprocal, due to mathematical restrictions (the relative numbers of known and unknown variables and stability of the model) we only included unidirectional paths. We also excluded V2 for simplicity. Figure 3 gives an overview of the simple structural model used. The time-series for each region was normalized to zero mean and unit variance. To assess effective connectivity in a condition-specific fashion, we used time-series that comprised observations during the condition in question. Path coefficients for both conditions ('attention' and 'no attention') were estimated using a maximum likelihood function with the software package AMOS (Amos for Windows, version 3.5, SmallWaters Corp., Chicago, IL). The covariance matrices used were calculated on the basis of 96 observations for 'attention' and 'no attention'. The variance of the residual influences were estimated but their path coefficients were constrained to be unity to reduce the number of estimated parameters (McIntosh *et al.*, 1994). Different (stacked) models were compared to assess the significance of changes due to attention: restricted models, in which either the path from V1 to V5 or from V5 to PP were forced to be equal for

Figure 3. Linear structural model for the dorsal visual stream. A sketch of the simplified model of the dorsal visual pathway, tested with structural equation modelling. Note that only unidirectional paths are included.

Table 2
Estimates of path coefficients for the linear model

(A) Subject 1

Connections		V1 $\rightarrow$ V5	$\rightarrow$ PP
		Path coefficients (standardized path coefficients)	
Right	attention	0.91 (0.90)	0.90 (0.78)
	no attention	0.56 (0.76)	0.30 (0.25)
Left	attention	0.88 (0.87)	0.52 (0.48)
	no attention	0.66 (0.76)	−0.05 (−0.03)
Right	χ^2 (P value)	25 (<0.01)	17 (<0.01)
Left	χ^2 (P value)	8 (<0.01)	8.5 (<0.01)

(B) Subject 2

Connections		V1 $\rightarrow$ V5	$\rightarrow$ PP
		Path coefficients (standardized path coefficients)	
Right	attention	0.74 (0.71)	0.63 (0.62)
	no attention	0.49 (0.61)	0.28 (0.30)
Left	attention	0.98 (0.95)	0.87 (0.87)
	no attention	0.81 (0.89)	0.37 (0.49)
Right	χ^2 (P value)	6.1 (<0.01)	8.1 (<0.01)
Left	χ^2 (P value)	10 (<0.01)	33 (<0.01)

(C) Subject 3

Connections		V1 $\rightarrow$ V5	$\rightarrow$ PP
		Path coefficients (standardized path coefficients)	
Right	attention	0.95 (0.70)	0.74 (0.73)
	no attention	0.56 (0.55)	0.49 (0.51)
Left	attention	0.89 (0.80)	0.67 (0.56)
	no attention	0.75 (0.79)	0.17 (0.19)
Right	χ^2 (P value)	8.5 (<0.01)	5.1 (<0.05)
Left	χ^2 (P value)	2.6 (=0.1)	13 (<0.01)

Unstandardized and standardized path coefficients for the model of Figure 3 comparing 'attention' and 'no attention' for both hemispheres. Statistical inference for each path is based on the lack of fit χ^2 value (see Materials and Methods). The comparison of path coefficients between 'attention' and 'no attention' shows marked changes in the connection between V1 and V5 and between V5 and PP. The χ^2 statistic indicated that freeing the path coefficients for 'attention' and 'no attention' leads to a highly significant improvement of fit.

attention and no attention and a corresponding free model in which these path coefficients were allowed to differ were compared. The null hypothesis was that freeing the parameters between the conditions does not significantly improve the fit.

Table 2 shows the path coefficients for 'attention' and 'no attention' for all three subjects. The table also shows the statistical inference based on the stacked model approach. Comparing path coefficients between 'attention' and 'no attention' shows marked changes in the connection between V5 and PP and to a lesser degree between V1 and V5. The χ^2 statistic indicated that allowing for different path coefficients between 'attention' and 'no attention' leads to a highly significant improvement of fit in both cases ($P < 0.05$). In other words attention can be construed as significantly modulating these connections.

Modelling Modulation by Interaction Terms — A Unified Approach

The linear path models of the previous section comparing 'attention' and 'no attention' revealed increased effective connectivity in the dorsal visual pathway in relation to attention. The question that arises is which part of the brain is capable of modulating these pathways? Based on lesion studies (Lawler and Cowey, 1987) and on the system for directed attention as described by Mesulam (Mesulam, 1990; Morecraft *et al.*, 1993), the dorsolateral prefrontal cortex or the anterior cingulate were candidates for such a modulatory role (only the right dorsolateral prefrontal cortex showed a significant activation during 'attention' relative to 'no attention').
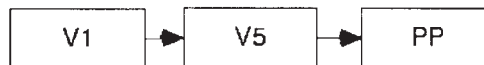
Selemon and Goldman-Rakic (1988) have shown that the prefrontal cortex is connected to many cortical areas implicated in spatially related behaviour and attention. They also note that prefrontal projections throughout the cortex terminate in layer I. This pattern is typical of feedback connections (Rockland and Pandya, 1979; van Essen and Maunsell, 1983). Therefore the prefrontal projections to PP have both the macro- and micro-anatomical characteristics of a modulatory projection system.

The right prefrontal region was included in our model as a moderator variable modulating the posterior visual pathway. Given the neuroanatomical projection from PFC to PP, we included a modulation of the pathway between V5 and PP: assuming a non-linear modulation of this connection, we included an interaction term $I_{V5,PFC}$ in our analysis. This vector, mediating the interaction, simply comprises the time-series of region V5 multiplied by the time-series of the right prefrontal cortex (orthogonalized according to equation 1). The influence of this variable on PP corresponds to the influence of the prefrontal cortex on the connection between V5 and PP. The interaction model is shown in Figure 4. Because our interaction model could accommodate changes in connectivity between 'attention' and 'no attention' the entire time-series was analysed (i.e. attention-specific changes are explicitly modelled). The covariance matrix subject to this analysis was based on 360 observations.

As we used the whole time-series in this model, we incorporated a further variable, accounting for sensory input to all exogenous variables (i.e. variables that do not receive input from other variables in the model). This dummy variable contained ones whenever visual stimulation was present and zeros during the 'fixation dot' condition.

As described in the linear model, we tested for the significance of the interaction effect by comparing a restricted and free model. In the restricted model the interaction term (i.e. path from $I_{V5,PFC}$ to PP) was set to zero. Table 3 shows the path coefficients and the χ^2 difference test for the interaction term and the main effect of the prefrontal cortex. All interaction terms were significant ($P < 0.05$). As there is a substantial anatomical connection between PP and PFC we also tested a model incorporating reciprocal connections between PP and PFC. In all three subjects this model was stable but showed only marginally different results: slightly higher significance of the interaction; slightly lower significance of the main effects. However, all effects remained significant at $P < 0.05$.

Testing the Impact of PFC on the Connectivity Between V5 and PP Using Regression Analysis

The presence of an interaction effect of the PFC on the connection between V5 and PP can also be illustrated by a simple regression analysis. If PFC shows a positive modulatory influence on the path between V5 and PP, the influence of V5 on PP should depend on the activity of PFC. This can be visualized by splitting the observations into two sets, one with observations in which PFC activity is high and another one in which PFC activity is low (cf. Friston *et al.*, 1995e). It is now
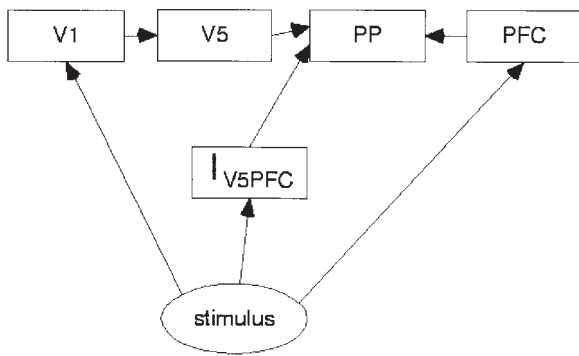
Figure 4. Structural model for the dorsal visual stream including the dorsolateral prefrontal cortex. A sketch of the extended model of the dorsal visual pathway with the modulatory influence of the prefrontal cortex (PFC) on the connection between V5 and PP.The main effect of PFC is also included to show whether the interaction is significant in the presence of the main effect. As opposed to the linear model, the stimulus is included to have an influence on all variables, that receive no input from within the model (i.e. exogenous variables V1, PFC, $I_{V5, PFC}$).

possible to perform separate regressions of PP on V5 for both sets. If the hypothesis of a positive modulation is true, the slope of the regression of PP on V5 should be steeper under high values of PFC. Figure 5 shows exactly this in all three subjects and provides the regression coefficients for the split-data. The *F* statistics and associated *P* values reflect the significance of the interaction term (V5 × PFC), in the presence of the two main effects (V5 and PFC) in the following regression model:

$$PP = b_1 \, V5 + b_2 \, PFC + b_3 \, V5 \times PFC \tag{2}$$

Regional Specificity
In this section we address the regional specificity of the interaction. This effect can be seen as the contribution of the interaction between two areas (V5 and PFC) in explaining the variation of activity in a third (PP). In this context a modulatory effect of PFC on the efferent projections from V5 would be expressed as a contribution from V5 that depended on activity in PFC. If the connection between V5 and PP is modulated by the PFC, the time-series of $I_{V5,PFC}$ (the orthogonalized product of the V5 and PFC time-series) should predict a component of the activity in the PP. To test this hypothesis we used the interaction term $I_{V5,PFC}$ as a regressor or explanatory variable and tested for the significance of the regression using a conventional SPM{*Z*} analysis. Figure 6 and Table 4 show the SPM{*Z*}s overlaid on a structural MRI and the coordinates for all three subjects. Subjects 2 and 3 showed the most significant effect in the right parietal cortex. Interestingly, in subject 1 the voxel with the most significant positive regression was found in the left parietal region, followed by the right parietal region. The regional specificity and reproducibility of this effect is remarkable.

Discussion
In this paper modulation of the dorsal visual pathway serves as an example of interactions in structural equation modelling in fMRI. We adopted a conservative modelling approach, where most regions were defined *a priori*, based on primate electro-physiological studies and human functional imaging studies (Zeki *et al.*, 1991; Tootell *et al.*, 1995). Motion perception has been well studied and critical areas have been identified in

Table 3
Estimates of path coefficients for the interaction model

(A) Subject 1

Paths		V5 → PP Path coefficients	$I_{V5,PFC}$ → PP	PP → PFC
Right		0.46	0.16	0.33
	χ^2 (*P* value)	–	4.6 (<0.05)	34.6 (<0.01)

(B) Subject 2

Paths		V5 → PP Path coefficients	$I_{V5,PFC}$ → PP	PP → PFC
Right		0.52	0.31	0.56
	χ^2 (*P* value)	–	10.1 (<0.05)	43.7 (<0.01)

(C) Subject 3

Paths		V5 → PP Path coefficients	$I_{V5,PFC}$ → PP	PP → PFC
Right		0.56	0.25	0.43
	χ^2 (*P* value)	–	33.2 (<0.01)	111.7 (<0.01)

Unstandardized path coefficients for the model in Figure 5 for both hemispheres. Only the path coefficients affecting the parietal cortex (PP) are shown. The χ^2 statistics for the effect of the interaction term (the multiplied time-series of V5 and the prefrontal cortex [PFC]), and for the main effect of PFC are shown. It can be seen that both, the direct effect from the PFC as the interaction ($I_{V5, PFC}$) are significant.

primates and man. Furthermore it is known that attention can modulate activity in the dorsal visual pathway at the level of V5 (Beauchamp and DeYoe, 1996; Treue and Maunsell, 1996; O'Craven and Savoy, 1997;) and PP (Beauchamp and DeYoe, 1996). The anterior cingulate and the prefrontal cortex are thought to exert a modulatory influence on visual connections. However, it transpired that the only region showing significant attention-specific activations in our data was the right dorso-lateral prefrontal cortex. The prefrontal cortex is known to play a special role in regulating the interplay of cortical regions (Shallice 1988). This has also been shown in the context of attention in patients with prefrontal lesions (Pierrot Deseilligny *et al.*, 1986). In terms of effective connectivity McIntosh and colleagues have demonstrated feedback from Brodmann area 46 to the dorsal visual pathway during spatial vision (McIntosh *et al.*, 1994). It is also interesting to note that in their model, which included interhemispheric connections, the influence of the right prefrontal region often dominated over the left prefrontal region.

Modulation
Modulation is an extremely flexible mechanism, especially on a small timescale, that may be critical for attention. In a mathematically and biologically compelling model Olshausen and colleagues (Olshausen *et al.*, 1993) have used the concept of modulation to simulate involuntary shifts of attention between objects in a given visual scene. As a possible mechanism for modulation, or gating, at the neuronal level they propose voltage-gated calcium channels (Llinas, 1988), that enable non-linear coupling between inputs. This has been shown for synaptic inputs into layer I of neocortex (Cauller and Connors, 1992), which supports the conjecture that attentional modulation could be exerted by prefrontal afferents, because prefrontal connections terminate predominantly in layer I. The modulation of the connection between V5 and PP by prefrontal influences might therefore be mediated by a change in synaptic efficacy underpinned by voltage-dependent calcium channels activated by prefrontal afferents.

The modulatory influence of the prefrontal cortex in our
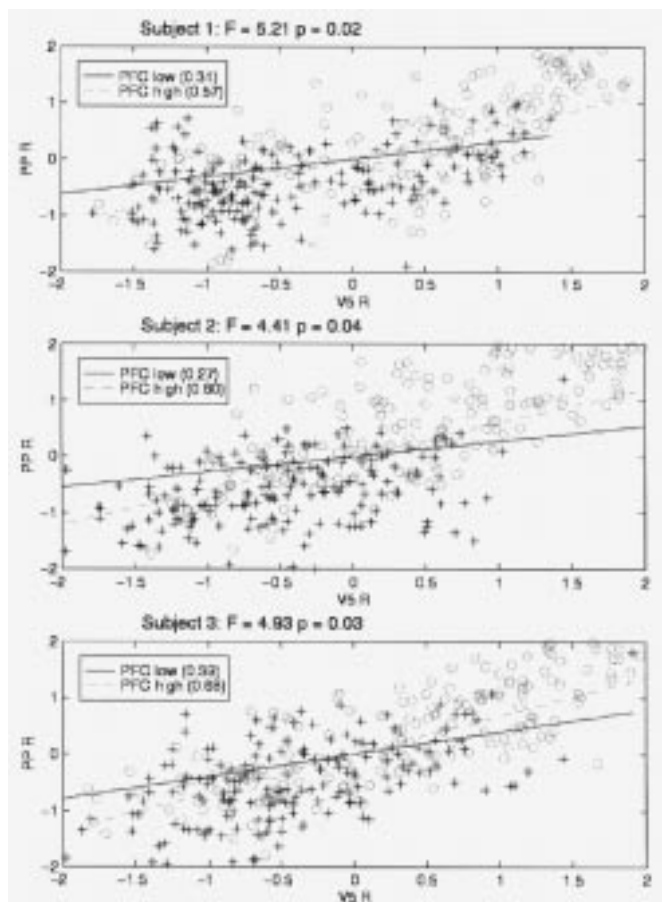
Figure 5. Regression between V5 and PP as a function of PFC activation. An alternative way of showing the modulatory effect of the PFC on the connection between V5 and PP. All observations were divided into two groups: one with observations in which PFC activity is high, one in which PFC activity is low. The graphs show separate regression curves for both groups. The F statistics and associated P values reflect the significance of the interaction term (V5 $\times$ PFC), in the presence of the two main effects (V5 and PFC) of the following regression model: PP $= b_1$ V5 $+ b_2$ PFC $+ b_3$ V5 $\times$ PFC.

Table 4
Regional specificity of the interaction

Subject	Location	Z score (P value, corrected)	x, y, z in mm
1	(1) parietal L	6.2 (<0.05)	−30, -57, 63
	(3) parietal R	6.0 (<0.05)	18, −69, 60
2	(1) parietal R	6.0 (<0.05)	30, −36, 63
	(2) Parietal R	5.4 (<0.05)	18, −57, 63
3	(1) Parietal R	5.5 (<0.05)	48, −42, 63

Z scores, corrected P values and coordinates for the significant regressions of the interaction effect $I_{V5,PFC}$. The numbers in front of the region denote the rank of significance. In subjects 2 and 3, the highest correlation was found in the right parietal cortex. In subject 1, the voxel with the most significant positive correlation was found in the left parietal region, followed by the right parietal region.

Figure 6. Regional specificity of the interaction term. SPM$\{Z\}$ overlaid on the individual's structural MR, assembling voxels showing a significant regression with the product of V5 and PFC. The threshold was set to $P < 0.0001$ (uncorrected). In subjects 2 and 3, the most significant correlation was found in the right parietal cortex (30, −36, 63 mm and 48, −42, 63 mm). In subject 1, the voxel with the most significant positive correlation was found in the left parietal region (−30, −57, 63 mm), followed by the right parietal region (18, −57, 63 mm). Locations are in reference to the anterior comissure.
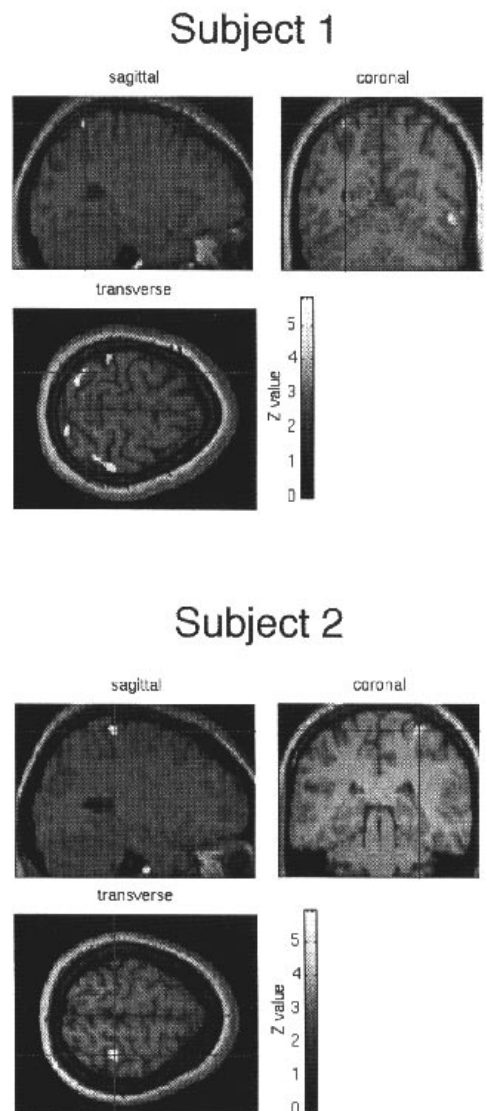
Subject 1

Subject 2
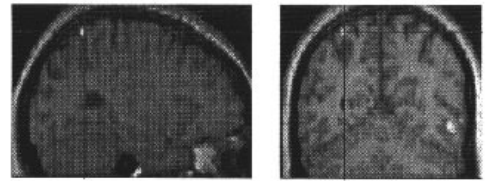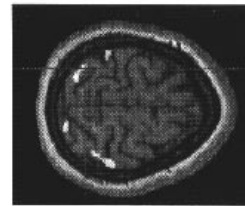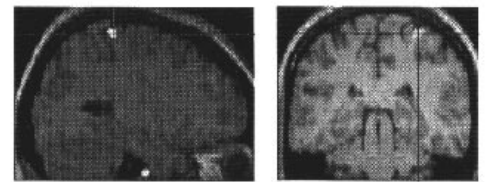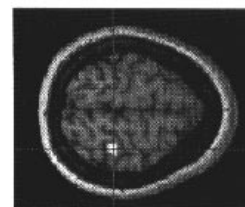
Subject 3
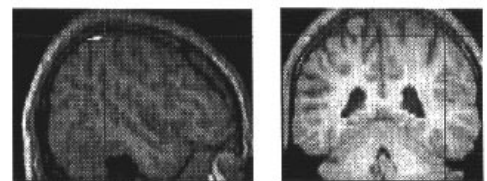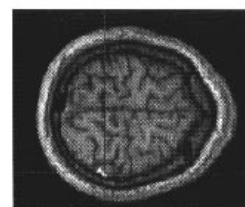
model was restricted to the connection between V5 and PP. However, the connection between V1 and V5 also exhibited a change in effective connectivity (Table 2). We did not include a similar modulatory interaction term at this level; however, it would be interesting to extend the existing model to allow for a similar interaction (i.e. V1 → V5 modulated by PP).

Structural Model of Posterior Visual Pathway

Our anatomical model represents a simple version of the dorsal visual pathway. This model has been used in an application of structural equation modelling to PET data (McIntosh *et al.*, 1994), where different connectivity patterns for spatial and object vision were demonstrated. Our analysis, which was restricted to the posterior visual pathway, showed changes of effective connectivity *within* a given system attributable to attentional modulation. We also demonstrated modulation of cortical connections by prefrontal cortex, using interaction terms. This technique could also be applied to model non-linear effects between two areas (e.g. intrinsic modulation). This can be seen as the interaction (e.g. non-linear bias) of a region with its afferents. This effect has been shown previously in the connectivity between V1 and V2 in fMRI (Friston *et al.*, 1995e).

Regional Specificity

The maximum *Z*-score pertaining to the regionally specific interaction effects was located in the parietal cortex, but did not exactly coincide with the regions included in our model (e.g. subject 3). This highlights the simplifying nature of models. It is likely that the parietal regions defined in our model are further subdivided and subserve different functions.

An important aspect of this analysis is that there is an entirely equivalent and symmetric interpretation of the physiological interactions above, namely that they reflect a modulation of PFC → PP connections by V5 activity. This is because an interaction can be construed as either a modulation of the effects of the first factor by the second, or equivalently a modulation of the second's effects by the first. There is no formal distinction between what is an effect and what is a modulatory factor. The potential for V5 modulation has anatomical support since it does project to the prefrontal cortex (Ungerleider and Desimone, 1986). However, our explanation that PFC modulates the connection between V5 and PP as an example of top-down modulation is more likely, given data that support an executive role for the prefrontal cortex (Pierrot Deseilligny *et al.*, 1986; Shallice, 1988). Furthermore it has been shown recently in a PET study that a region within 10 mm of our prefrontal region is involved in attentional processing in the context of object categorization (Rees *et al.*, 1997)

Comparison with Other Structural Equation Modelling Studies

Structural equation modelling has been used to show interesting changes in effective connectivity in the motor system (Grafton *et al.*, 1994) and in the visual system (McIntosh *et al.*, 1994) using PET. However, in PET studies the number of observations is restricted by the radiation exposure. To achieve a reasonable sensitivity, the data of the studies cited had to be pooled over subjects, which can introduce a confounding effect, as it is difficult to distinguish between variance introduced by the subjects (e.g. severity of disease) or the task itself (Grafton *et al.*, 1994). fMRI offers a unique advantage over PET in this respect, as it provides sufficient data to assess effective connectivity in single subjects. However, one is then faced with the problem of
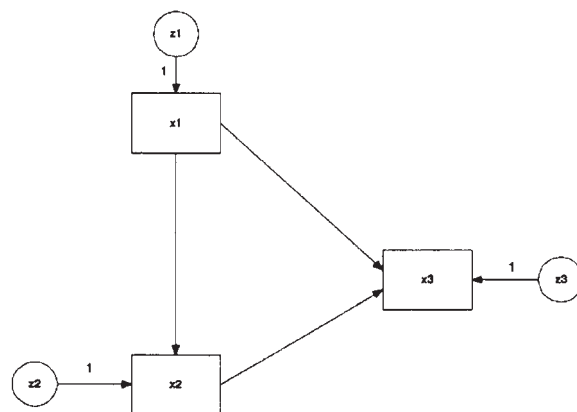

Figure 7. Path model example. Simple path model including three measured variables. Variables *x* are 'caused' by a set of independent variables *z*. This could also be construed as a set of variables *x* with residual influences *z* (outside the model). Variables *x* also cause each other.

generalizing the results to the population from which the subject was selected. Both group and single subject analyses may be confounded if task responses change due to factors that are not central to investigation, such as adaptation, fatigue or anomalous task responses.

Connectivity versus Categorical Analyses

One obvious advantage of the assessment of effective connectivity is that it allows one to test hypotheses about the integration of cortical areas. For example, the categorical comparison between 'attention' and 'no attention' revealed prestriate, parietal and frontal activations. However, the only statement possible is that these areas show higher rCBF during the 'attention' condition as opposed to the 'no attention' condition. The analysis of effective connectivity revealed two additional results. Firstly, we showed, that attention predominantly affects the pathway from V1 to V5 and from V5 to PP. Secondly, the introduction of non-linear interaction terms allowed us to test the hypothesis about how these modulations are mediated. The latter analysis suggested that the prefrontal cortex exerts a modulatory influence on posterior cortical areas.

Conclusion

Structural equation modelling applied to fMRI data revealed marked changes in effective connectivity in the posterior visual pathway in relation to attentional set. Furthermore the introduction of non-linear interaction terms allowed us to model a modulatory influence from the dorsolateral prefrontal cortex on this pathway. These results were not evident from categorical comparisons. We hope that the assessment of effective connectivity will be useful in a variety of imaging experiments in which one hypothesises changes in effective connectivity under different experimental conditions.

Appendix

Mathematical Implementation of Structural Equation Modelling

Structural equation modelling minimizes the difference between the observed **S** and implied covariance matrix Σ. The variance–covariance structure **S** of the observed variables is given by:

$$\mathbf{S} = (1/(N-1)).\mathbf{x}^T.\mathbf{x} \qquad (3)$$

where $\mathbf{x}$ is a $N \times p$ matrix of deviation (from the mean) scores of the p observed variables with N observations and $\mathbf{x}^T$ is $\mathbf{x}$ transpose. The matrix $\mathbf{S}$ is symmetric with the sample variances down its main diagonal and the covariances off the diagonal.

Consider a model where the variables $\mathbf{x}$ are 'caused' by a set of independent variables $\mathbf{z}$ (Fig. 7). This could also be construed as a set of variables $\mathbf{x}$ with residual influences $\mathbf{z}$ (outside the model). In addition the variables $\mathbf{x}$ may cause each other.

Algebraically, the model for $\mathbf{x}$ is:

$$\mathbf{x}.\mathbf{I} = \mathbf{x}.\mathbf{B} + \mathbf{z} \qquad (4)$$

where $\mathbf{B}$ is a matrix of unidirectional path coefficients and $\mathbf{I}$ is the identity matrix. Here $\mathbf{x}$ appears on both sides of the equation. This reduces to

$$\mathbf{x} = \mathbf{z}.\mathrm{inv}(\mathbf{I} - \mathbf{B}) \qquad (5)$$

Looking at the variance–covariance structure implied by the model and omitting the denominator $1/(N-1)$ we have:

$$\mathbf{x}^T.\mathbf{x} = \Sigma = (\mathbf{z}.\mathrm{inv}(\mathbf{I} - \mathbf{B}))^T.(\mathbf{z}.\mathrm{inv}(\mathbf{I} - \mathbf{B}))$$
$$= \mathrm{inv}(\mathbf{I} - \mathbf{B})^T.\mathbf{C}.(\mathrm{inv}(\mathbf{I} - \mathbf{B})) \qquad (6)$$

where $\mathbf{C} = \mathbf{z}^T.\mathbf{z}$.

$\mathbf{B}$ is not symmetric because of asymmetric connections. $\mathbf{C}$ (variance–covariance structure of $\mathbf{z}$) is a diagonal matrix and contains the residual variances. If interactions among the residual influences were to be incorporated into the model, their covariances would appear (symmetrically) off the leading diagonal in $\mathbf{C}$ (not shown in Fig. 7). $\mathbf{x}^T.\mathbf{x}$ is the implied variance–covariance structure Σ. Parameters in the matrices $\mathbf{C}$ and $\mathbf{B}$ are called free parameters. The free parameters are estimated by minimizing a function of $\mathbf{S}$ and Σ. To date the most widely used objective function for structural equation modelling is the maximum likelihood (ML) function (Bollen, 1989):

$$F_{ML} = \log |\Sigma| + \mathrm{tr}(\mathbf{S}.\mathrm{inv}(\Sigma)) - \log|\mathbf{S}| - p \qquad (7)$$

where $\mathrm{tr}(.)$ is the trace of the matrix and p is the number of free parameters. The Newton–Raphson or other gradient descent methods are used to estimate the parameters. Starting values can be provided for the free parameters or estimated by ordinary least squares (McIntosh and Gonzalez-Lima, 1994).

Weighted Least Squares

If the data do not conform to multinormal distributional assumptions, then the objective function to minimize (instead of F_{ML}) becomes:

$$F_{WLS} = [\mathbf{s} - \sigma(\theta)]^T \mathbf{W}^{-1} [\mathbf{s} - \sigma(\theta)] \qquad (8)$$

where $\mathbf{s}$ is a vector of $1/2(p+q)(p+q+1)$ unique elements of $\mathbf{S}$, $\sigma(\theta)$ is the corresponding vector of $\Sigma(\theta)$ obtained from equation (6), and θ are the t free parameters. Values of θ are selected so as to minimize F_{WLS}, the weighted sum of squared deviations $\mathbf{s}$ from $\sigma(\theta)$. WLS in structural equation modelling is similar to WLS in multiple linear regression. The only difference is that one is minimizing differences between the expected and observed covariances rather than using the individual observations. If $\mathbf{W}$ is the identity matrix, this reduces to ordinary least squares

estimates. In our case the matrix $\mathbf{W}$ is a consistent estimator of the limiting covariance matrix of $n^{1/2}(\mathbf{s} - \sigma(\theta))$, where n equals the number of observations minus 1 (Browne, 1984).

References
Aertsen A, Preissl H (1991) Dynamics of activity and connectivity in physiological neuronal networks. New York: VCH.

Assad JA, Maunsell JH (1995) Neuronal correlates of inferred motion in primate posterior parietal cortex. Nature 373:518–521.

Beauchamp MS, DeYoe EA (1996) Brain areas for processing motion and their modulation by selective attention. NeuroImage 3(Supplement):S245.

Bollen KA (1989) Structural equations with latent variables. New York: John Wiley.

Browne MW (1984) Asymptotic distribution free methods in analysis of covariance structures. Br J Math Statist Psychol 37:62–83.

Bushnell MC, Goldberg ME, Robinson DL (1981) Behavioral enhancement of visual responses in monkey cerebral cortex. I. Modulation in posterior parietal cortex related to selective visual attention. J Neurophysiol 46:755–772.

Corbetta M, Miezin FM, Dobmeyer S, Shulman GL, E. P. S. (1991) Selective and divided attention during visual discrimination of shape, color, and speed: functional anatomy by positron emission tomography. J Neurosc 13:1202–1226.

Coull JT, Frith CD, Frackowiak RSJ, Grasby PM (1996) A fronto-parietal network for rapid visual information processing: a PET study of sustained attention and working memory. Neuropsychologia (in press).

Evans AC, Collins DL, Mills SR, Brown ED, Kelly RL, Peters TM (1993) 3D statistical neuroanatomical models from 305 MRI volumes. Proc IEEE Nuclear Science Symposium and Medical Imaging, pp 1813–1817.

Friston KJ, Ashburner J, Frith CD, Poline J-B, Heather JD, Frackowiak RSJ (1995a) Spatial registration and normalization of images. Hum Brain Mapping 2:1–25.

Friston KJ, Frith CD, Frackowiak RSJ (1993a) Time-dependent changes in effective connectivity measured with PET. Hum Brain Mapping 1:69–80.

Friston KJ, Frith CD, Liddle PF, Frackowiak RSJ (1993b) Functional connectivity: the principal component analysis of large (PET) data sets. J Cereb. Blood Flow Metab 13:5–14.

Friston KJ, Frith CD, Turner R, Frackowiak RSJ (1995b) Characterizing evoked hemodynamics with fMRI. NeuroImage 2:157–165.

Friston KJ, Holmes AP, Poline J-B, Grasby PJ, Williams SCR, Frackowiak RSJ, Turner R (1995c) Analysis of fMRI time-series revisited. NeuroImage 2:45–53.

Friston KJ, Holmes AP, Worsley KP, Poline J-B, Frith CD, Frackowiak RSJ (1995d) Statistical parametric maps in functional imaging: a general linear approach. Hum Brain Mapping 2:189–210.

Friston KJ, Ungerleider LG, Jezzard P, Turner R (1995e) Characterizing modulatory interactions between V1 and V2 in human cortex with fMRI. Hum Brain Mapping 2:211–224.

Friston KJ, Holmes AP, Ashburner J, Poline J-B (1996) SPM96. World Wide Web http://www.fil.ion.ucl.ac.uk/spm.

Gerstein GL, Bedenbaugh P, Aertsen A (1989) Neuronal assemblies. IEEE Trans Biomed Enging 36:4–14.

Gerstein GL, Perkel DH (1969) Simultaneously recorded trains of action potentials: analysis and functional interpretation. Science 164:828–830.

Gochin PM, Miller EK, Gross CG, Gerstein GL (1991) Functional interactions among neurons in inferior temporal cortex of the awake macaque. Exp Brain Res 84:505–516.

Grafton ST, Sutton J, Couldwell W, Lew M, Waters C (1994) Network analysis of motor system connectivity in Parkinson's disease: modulation of thalamocortical interactions after pallidotomy. Hum Brain Mapping 2:45–55.

Horwitz B, Grady C, Haxby J, Schapiro M, Carson R, Herscovitch P,

Ungerleider L, Mishkin M, Rapoport S (1991) Object and spatial visual processing: intercorrelations of regional cerebral blood flow among posterior brain regions. J Cereb Blood Flow Metab 11:S380.

Kenny DA, Judd CM (1984) Estimating nonlinear and interactive effects of latent variables. Psychol Bull 96:201–210.

La Berge D (1995) Attentional processing. Cambridge, MA: Harvard University Press.

Lagreze HL, Hartmann A, Anzinger G, Shaub A, Deister A (1993) Functional cortical interaction patterns in visual perception and visuospatial problem solving. J Neurol Sci 114:25–35.

Lawler KA, Cowey A (1987) On the role of posterior parietal and prefrontal cortex in visuo-spatial perception and attention. Exp Brain Res 65:695–698.

McIntosh AR, Gonzalez-Lima F (1991) Structural modelling of functional neural pathways mapped with 2-deoxyglucose: effects of acoustic startle habituation on the auditory system. Brain Res 547:295–302.

McIntosh AR, Gonzalez-Lima F (1994) Structural equation modelling and its application to network analysis in functional brain imaging. Hum Brain Mapping 2:2–22.

McIntosh AR, Bookstein FL, Haxby JV, Grady CL (1996a) Spatial pattern analysis of functional brain images using partial least squares. NeuroImage 3:143–157.

McIntosh AR., Grady CL, Haxby JV, Ungerleider LG, Horwitz B (1996b) Changes in limbic and prefrontal functional interactions in a working memory task. Cereb Cortex 6:571–584.

McIntosh AR, Grady CL, Ungerleider LG, Haxby JV, Rapoport SI, Horwitz B (1994) Network analysis of cortical visual pathways mapped with PET. J Neurosci 14:655–666.

Mesulam MM (1981) A cortical network for directed attention and unilateral neglect. Ann Neurol 10:309–325.

Mesulam MM (1990) Large-scale neurocognitive networks and distributed processing for attention, language, and memory. Ann Neurol 28:597–613.

Morecraft RJ, Geula C, Mesulam MM (1993) Architecture of connectivity within a cingulo-fronto-parietal neurocognitive network for directed attention. Arch Neurol 50:279–284.

Mountcastle VB, Andersen RA, Motter BC (1981) The influence of attentive fixation upon the excitability of the light-sensitive neurons of the posterior parietal cortex. J Neurosci 1:1218–1225.

Nyberg L, McIntosh AR, Cabeza R, Nilsson L-G, Houle S, Habib R, Tulving E (1996) Network analysis of positron emission tomography regional cerebral blood flow data: ensemble inhibition during episodic memory retrieval. J Neurosci 16:3753–3759.

O'Craven KM, Rosen BR, Kwong KK, Treisman A, Savoy RL (1997) Voluntary attention modulates fMRI activity in human MT–MST. Neuron 18:591–598.

Pierrot Deseilligny C, Gray F, Brunet P (1986) Infarcts of both inferior parietal lobules with impairment of visually guided eye movements, peripheral visual inattention and optic ataxia. Brain 109:81–97.

Rees G, Frackowiak R, Frith C (1997) Two modulatory effects of attention that mediate object categorization in human cortex. Science 275:835–838.

Rizzolatti G, Riggio L, Dascola I, Umilta C (1987) Reorienting attention across the horizontal and vertical meridians: evidence in favour of a premotor theory of attention. Neuropsychologia 25:31–40.

Rockland KS, Pandya DN (1979) Laminar origins and terminations of cortical connections of the occipital lobe in the rhesus monkey. Brain Res 179:3–20.

Sadasivan PK, Dutt DN (1996) SVD based technique for noise reduction in electroencephalographic signals. Signal Process 55:179–189.

Selemon LD, Goldman Rakic PS (1988) Common cortical and subcortical targets of the dorsolateral prefrontal and posterior parietal cortices in the rhesus monkey: evidence for a distributed neural network subserving spatially guided behavior. J Neurosci 8:4049–4068.

Shallice T (1988) From neuropsychology to mental structure. Cambridge: Cambridge University Press.

Talairach P, Tournoux J (1988) A stereotactic coplanar atlas of the human brain. Stuttgart: Thieme Verlag.

Tootell RB, Reppas JB, Kwong KK, Malach R, Born RT, Brady TJ, Rosen BR, Belliveau JW (1995) Functional analysis of human MT and related visual cortical areas using magnetic resonance imaging. J Neurosci 15:3215–3230.

Treue S, Maunsell HR (1996) Attentional modulation of visual motion processing in cortical areas MT and MST. Nature 382:539–541.

Ungerleider LG, Desimone R (1986) Cortical connections of visual area MT in the macaque. J Com Neurol 248:190–222.

van Essen DC, Maunsell JHR (1983) Hierarchical organization and functional streams in the visual cortex. Trends Neurosci 6:370–375.

Vandenberghe R, Dupont P, De Bruyn B, Bormans G, Michiels J, L. M., Orban GA (1996) The influence of stimulus location on the brain activation pattern in detection and orientation discrimination. A PET study of visual attention. Brain 119:1263–1276.

Watson D, Myers R, Frackowiak RS, Hajnal JV, Woods RP, Mazziotta JC, Shipp S, Zeki S (1993) Area V5 of the human brain: evidence from a combined study using positron emission tomography and magnetic resonance imaging. Cereb Cortex 3:79–94.

Worsley KJ, Friston KJ (1995) Analysis of fMRI time-series revisited — again. NeuroImage 2:173–181.

Zeki S, Watson JD, Lueck CJ, Friston KJ, Kennard C, Frackowiak RS (1991) A direct demonstration of functional specialization in human visual cortex. J Neurosci 11:641–649.